Eur. Phys. J. D **19**, 421–427 (2002)
DOI: 10.1140/epjd/e20020084

THE EUROPEAN PHYSICAL JOURNAL D
EDP Sciences

Intensity noise of injected Nd:YVO_4 microchip lasers

A. Bramati[a], J.-P. Hermier, V. Jost, and E. Giacobino

Laboratoire Kastler Brossel, Université Pierre et Marie Curie, École Normale Supérieure, CNRS, 4 place Jussieu, 75252 Paris Cedex 05, France

Received 10 December 2001 and Received in final form 6 March 2002

Abstract. The combined effects of the pump noise suppression and injection locking technique on the intensity noise of a diode pumped Nd:YVO_4 microchip laser are theoretically and experimentally investigated. Complete cancellation of the relaxation oscillation peak is experimentally achieved. Very good agreement between experimental results and theoretical predictions of a fully quantum model describing lasers with injected signal is found.

PACS. 42.50.Dv Nonclassical field states; squeezed, antibunched, and sub-Poissonian states; operational definitions of the phase of the field; phase measurements – 42.55.Xi Diode-pumped lasers – 42.50.Lc Quantum fluctuations, quantum noise, and quantum jumps

1 Introduction

In recent years, intensity noise properties of various kind of lasers have been thoroughly investigated to the search of quiet light sources for applications in metrology, information technology and high precision interferometry [1–3]. Great interest has been focused on diode pumped solid state lasers such as Nd:YAG or Nd:YVO_4 lasers [4–11]. The intensity noise spectrum of these lasers is determined by two dominant factors: the noise of the pump mechanism (for frequencies below the relaxation oscillation) and the resonant relaxation oscillation. The first factor can be partially eliminated using solid state lasers pumped with amplitude squeezed diode lasers [9–11]. The second factor is usually eliminated by using a standard feedback control on the driving current of the pump laser diode. However, the use of a standard feedback loop (which usually has a maximum gain at zero frequency) can be shown to completely destroy (due to the coupling with the vacuum fluctuations) the quantum intensity noise features of the laser and cancel the advantages coming from the squeezed pump [12–16]. The injection locking of the laser constitutes a very efficient alternative technique: in fact it has been theoretically predicted and experimentally observed that the relaxation oscillation of the slave laser is overdamped when injection locking with an intensity-stabilised master laser is applied [7,8,17]. The cancellation of the relaxation oscillation peak is achieved without affecting the intensity noise features of the injected laser in the low frequency range. In this region, in fact, the intensity fluctuations of the laser are strongly coupled with the pump fluctuations [18] and the intensity noise performances are mainly determined by the noise of the pump mechanism. The combination of pump noise suppression and injection locking is hence a very promising technique which should allow to improve the noise performances of diode pumped solid state lasers: the elimination of the relaxation oscillation peak results in an efficient stabilisation of the intensity noise in the middle frequency region (megahertz range), while the suppression of pump noise should allow to achieve intensity noise reduction below the shot noise level as predicted by theoretical models.

To date some accurate theoretical and experimental investigation have been performed on the effects of pump noise [9–11,18] and injection locking [8] on intensity noise of solid state lasers. However, mainly due to technical limitations, no works addressed the experimental investigation of the combined effects of these techniques. In particular, no experimental studies combining pump noise suppression based on amplitude squeezed pump laser diode and injection locking by an intensity-stabilised master laser can be found in literature. Our work is the first attempt to experimentally access for solid state laser an operating regime in which non-classical effects could be relevant. The outline of the paper is as follows. In Section 2 we use a quantum model describing lasers with injected signal for theoretical investigation of the intensity noise properties of an injected Nd:YVO_4 microchip laser pumped by an amplitude squeezed diode laser; an analytical expression is derived for our specific laser which clearly shows the effects of injection locking. In Section 3 the experimental set-up is described. Finally, in Section 4, agreement between the experimental realisation and the assumptions of the model is discussed and the experimental results

[a] e-mail: bramati@spectro.jussieu.fr

are presented. Complete cancellation of the resonant relaxation oscillation is experimentally achieved and good agreement is found between experimental results and theoretical predictions.

2 Theory

For a theoretical description of the intensity noise properties of the injected solid state lasers, we have used a full quantum model based on the Langevin equations approach developed in [17]. The model considers a system of homogeneously broadened two-level atoms (assuming that the lower level is not the ground state) in resonant interaction with a mode of the electromagnetic field in a cavity of length L and volume V. The field in the cavity is driven by an external coherent optical signal, also resonant with the cavity mode. The laser dynamics is described by the following stochastic c-number Langevin equations deduced from the normally ordered operator Langevin equations for the same system, using the standard procedure:

$$\dot{\mathcal{A}}(t) = -\kappa/2\ \mathcal{A}(t) + g\mathcal{M}(t) + \kappa/2\ \lambda(t) + \mathcal{F}_\gamma(t) \tag{1}$$

$$\dot{\mathcal{M}}(t) = -\gamma_{ab}\mathcal{M}(t) + g\left[\mathcal{N}_a(t) - \mathcal{N}_b(t)\right]\mathcal{A}(t) + \mathcal{F}_\mathcal{M}(t) \tag{2}$$

$$\begin{aligned}\dot{\mathcal{N}}_a(t) = {} & R - (\gamma_a + \gamma_a')\mathcal{N}_a(t) \\ & -g\left[\mathcal{A}^*(t)\mathcal{M}(t) + \mathcal{M}^*(t)\mathcal{A}(t)\right] + \mathcal{F}_a(t)\end{aligned} \tag{3}$$

$$\begin{aligned}\dot{\mathcal{N}}_b(t) = {} & -\gamma_b\mathcal{N}_b(t) + \gamma_a'\mathcal{N}_a(t) \\ & +g\left[\mathcal{A}^*(t)\mathcal{M}(t) + \mathcal{M}^*(t)\mathcal{A}(t)\right] + \mathcal{F}_b(t).\end{aligned} \tag{4}$$

The stochastic c-number variable $\mathcal{A}(t)$ represents the electromagnetic field. $\lambda(t)$ represents the injected coherent optical signal. The injected field is assumed to be in a coherent state, this means that its fluctuations are equivalent to the vacuum fluctuations. In some case, this could limit the possibility to apply the model to describe a realistic experiment, since the master laser used for the injection locking may exhibit some excess noise. More general models dealing with arbitrary noise of the injected field have been developed [7]. However, we will show in next section that our experimental conditions meets very well the assumptions of the model. $\mathcal{N}_a$ and $\mathcal{N}_b$ represent the macroscopic atomic population of the upper and lower level respectively. $\mathcal{M}(t)$ represents the macroscopic atomic polarisation. κ is the total cavity damping constant: we assume a definition of κ that accounts for internal optical losses: $\kappa = \kappa_{\rm out} + \kappa_{\rm losses}$, where $\kappa_{\rm out}$ represents the output coupling, and $\kappa_{\rm losses}$ the internal optical losses. γ_a and γ_b are the decay rates of the populations of the upper and lower levels to other atomic levels; γ_a' is the spontaneous decay rate between the lasing levels and γ_{ab} is the decay rate of the atomic polarisation. R is the mean pumping rate. The constant g corresponds to the electric dipole coupling between the two-level atoms and the field. The functions $\mathcal{F}_k(t)$ with $k = \gamma, \mathcal{M}, a, b$ are the stochastic c-number Langevin forces with the properties:

$$\langle \mathcal{F}_k(t) \rangle = 0 \tag{5}$$

$$\langle \mathcal{F}_k(t)\mathcal{F}_l(t') \rangle = 2\mathcal{D}_{kl}\delta(t - t') \tag{6}$$

where $\mathcal{D}_{kl}$ represents the diffusion coefficient for the c-number Langevin force. The nonvanishing diffusion coefficients are given in the appendix [17].

The steady state is obtained from equations (1–4) by neglecting the fluctuation terms and setting the time derivatives equal to zero. Expressing the atomic variables in terms of the steady state field $\mathcal{A}_s$ one gets:

$$\mathcal{N}_{as} = \frac{R}{\gamma_a + \gamma_b} + \frac{\kappa\gamma_{ab}\gamma_b}{2g^2(\gamma_a + \gamma_b)}\left(1 - \frac{\lambda}{\mathcal{A}_s}\right) \tag{7}$$

$$\mathcal{N}_{as} - \mathcal{N}_{bs} = \frac{\kappa\gamma_{ab}}{2g^2}\left(1 - \frac{\lambda}{\mathcal{A}_s}\right) \tag{8}$$

$$\mathcal{M}_s = \frac{\kappa}{2g}\left(1 - \frac{\lambda}{\mathcal{A}_s}\right)\mathcal{A}_s \tag{9}$$

where the steady state field $\mathcal{A}_s$ is a solution of the equation

$$\lambda = \frac{I - I_0}{I + 1}\mathcal{A}_s\ . \tag{10}$$

I and I_0 represent the normalised intensity for the laser with and without an injected signal respectively. Their definitions are as follows:

$$I = \frac{|\mathcal{A}_s|^2}{|\mathcal{A}_{\rm sat}|^2}, \quad I_0 = \frac{|\mathcal{A}_0|^2}{|\mathcal{A}_{\rm sat}|^2} \tag{11}$$

where

$$|\mathcal{A}_{\rm sat}|^2 = \frac{\gamma_{ab}\gamma_b}{2g^2}\frac{\gamma_a + \gamma_a'}{\gamma_a + \gamma_b} \tag{12}$$

is the saturation intensity for the free-running laser ($\lambda = 0$) and

$$|\mathcal{A}_0|^2 = |\mathcal{A}_{\rm sat}|^2 (R/R_{\rm th} - 1) \tag{13}$$

is the steady state intensity for the free-running laser. $R_{\rm th}$ represents the threshold pumping rate for the free running laser given by

$$R_{\rm th} = k\frac{\gamma_{ab}\gamma_b}{2g^2}\frac{\gamma_a + \gamma_a'}{\gamma_b - \gamma_a'}\ . \tag{14}$$

By linearizing equations (1–4) around the steady state solutions and by applying the Fourier transform to the field and atomic variables, one gets a linear system of algebraic equations. Its solution allows to calculate analytically the intensity noise spectrum at the laser output as a function of the relaxation rates and the pump noise. The derived expression is quite general and does not rely on any adiabatic elimination of variables, hence it is suitable to describe any type of lasers. However, the laser under investigation in our experiment is a Nd:YVO_4 laser belonging to the third class lasers: for these lasers the decay rate of the atomic polarisation γ_{ab} is much faster than the other relaxation rates. In this condition, it is possible to perform an adiabatic elimination of the atomic polarisation and derive an approximate expression for the intensity noise spectrum at the laser output.

In the original formulation of the model [17] the pump noise is described by the parameter p ranging from 0 to 1 ($p = 0$ for Poissonian pump; $p = 1$ for regular pump). In order to reproduce the experimental conditions more precisely, we generalize the model by introducing the spectral density of the pump noise $s(\tilde{\Omega})$ normalised to the shot noise.

According with [17], the normalised intensity noise spectrum at the laser output for a third class laser is given by:

$$V_{\rm out}(\tilde{\Omega}) = 1 + \eta \frac{2b(a+a')}{b-a'} \frac{1}{D(\tilde{\Omega})} \times \Bigg(\left(b^2 + \tilde{\Omega}^2\right) \left[(a+a')^2 + \tilde{\Omega}^2\right] \frac{n}{a+a'} + 2w^2 \Big\{ \left[(b-a')^2 + \tilde{\Omega}^2\right] \left[n + \left(s(\tilde{\Omega}) - 1\right) r/2\right] - \left[(b-a')(a+a') + \tilde{\Omega}^2\right] \left(r - \frac{a+2a'}{a+a'} n\right) + \left[(a+a')^2 + \tilde{\Omega}^2\right] \frac{a'}{a+a'} n \Big\} \Bigg) \quad (15)$$

where we set $p(\tilde{\Omega}) = 1 - s(\tilde{\Omega})$, and $\eta = \kappa_{\rm out}/\kappa$ represents the correction for internal optical losses. The dimensionless parameters a, b and the dimensionless noise frequency $\tilde{\Omega}$ are defined as follows:

- $a \equiv \gamma_a/\kappa$ (respectively $b \equiv \gamma_b/\kappa$) is the normalised decay rate of the upper level (respectively lower level);
- $a' \equiv \gamma_{a'}/\kappa$ is the normalised spontaneous decay rate between the lasing levels;
- $x \equiv \lambda/\mathcal{A}_s$; then x^2 corresponds to the ratio between the injected power and the power emitted by the laser;
- $\tilde{\Omega} \equiv \Omega/\kappa$.

We also used the following definitions:

$$D(\tilde{\Omega}) = \left| \left(\frac{1}{2}x - {\rm i}\tilde{\Omega}\right)(b - {\rm i}\tilde{\Omega})(a + a' - {\rm i}\tilde{\Omega}) + 2w^2(a + b - 2{\rm i}\tilde{\Omega})\left(1 - x/2 - {\rm i}\tilde{\Omega}\right)\right|^2 \quad (16)$$

$$n = \frac{r(a+a') + (b-a')(1-x)}{a+b} \quad (17)$$

$$w^2 = \frac{(a+a')b\,(r-1+x)}{2(a+b)\,(1-x)}. \quad (18)$$

The normalised pump parameter r is defined as the ratio between the pump power $p_{\rm pump}$ and the threshold pump power $p_{\rm th}$: $r = p_{\rm pump}/p_{\rm th}$. In order to gain some physical insight on effects of the injection on the intensity noise features of the laser from equation (15), we can make some approximations which lead to a more simplified formula. For the lasers under investigation the conditions $1 \gg b \gg a \gg a'$ are verified. Moreover, from the intensity noise spectrum of these lasers, shown in Figure 1, it is evident that the minimum intensity noise is found at zero frequency: setting $\tilde{\Omega} = 0$ in equation (15) and with the additional conditions $x, rx \ll 1$ usually verified in the experiment we derive the very simple following formula:

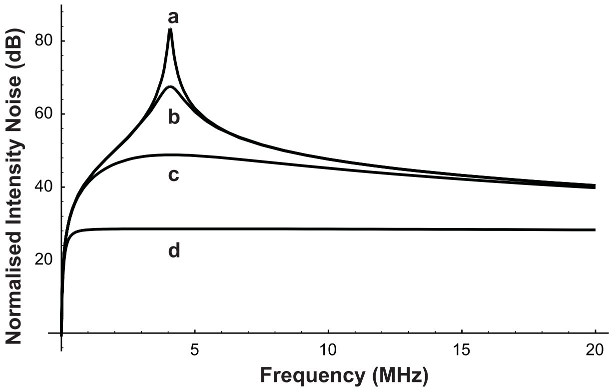

Fig. 1. Calculated normalised intensity noise spectra of the injected Nd:YVO$_4$ microchip laser with the parameters given in the Table 1 for different injected powers (curve a: $x = 0$, curve b: $x = 0.001$, curve c: $x = 0.01$, curve d: $x = 0.1$). The pump is assumed to be noiseless ($s = 0$). The normalised pump parameter is $r = 3$.

$$V_m(0) = 1 - \eta + \eta \left[s + \frac{s + 1 - 2x}{r - 1} + \frac{2(1-x)}{(r-1)^2} \right] \cdot \quad (19)$$

From equation (19) we can derive the condition for observing squeezing of the intensity noise at the laser output:

$$r > \frac{3 - s - 2x}{1 - s} \equiv r_{sq}. \quad (20)$$

Equation (20) indicates that intensity squeezing can only be observed with a squeezed pump ($s < 1$). The effect of the injection is also clearly indicated by equation (20): the normalised pump parameter r_{sq} which allows to generate squeezing in the injection locked laser is lower with respect to the corresponding value for the free running laser, obtained setting $x = 0$ in equation (20). Inspection of equation (19) clearly shows that the intensity noise of the laser decreases with the pump rate r and is limited by the overall quantum efficiency of the laser which accounts for internal optical losses and for efficiency of the pump mechanism. This behaviour is analogous to that exhibited by the free running laser, as we have pointed out in a previous work [11]. The role of the injection locking is also evident from equation (19): the intensity noise at zero frequency is less for the injected laser than for the free running one. This behaviour is confirmed by the predictions obtained from the general formula (15) as shown in Figure 2. In this figure we report the comparison, in the low frequency range, between the intensity noise spectra for the injected laser and for the free running laser. It is worth stressing that equations (19, 20) were derived in the limit $x, rx \ll 1$: taking into account typical experimental values of x (of the order of 0.1 or less), the previous condition implies that equations (19, 20) are good approximations (within 5%) of the general formula reported in equation (15) only for $r < 10$. Despite to the small range of validity, these equations cover all the experimentally accessible values for the normalised pump parameter r,

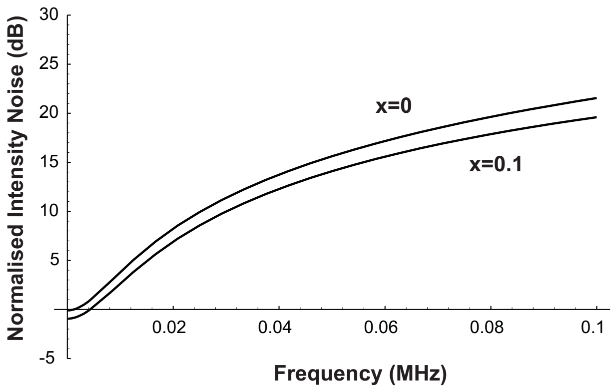

Fig. 2. Calculated normalised intensity noise spectra in the low frequency region for the injected ($x = 0.1$) and free running ($x = 0$) Nd:YVO_4 microchip laser. The parameters are given in the Table 1. The pump is assumed to be noiseless ($s = 0$). The normalised pump parameter is $r = 3$.

Table 1. Values of the laser parameters used for theoretical calculations.

Parameter	Value
γ_a	3.3×10^4 s^{-1}
γ'_a	3.3×10^3 s^{-1}
γ_b	10^9 s^{-1}
γ_{ab}	7×10^{11} s^{-1}
κ	9×10^9 s^{-1}
κ_{out}	8.36×10^9 s^{-1}

as we will show in next section. The intensity noise properties of the injected Nd:YVO_4 laser in the overall frequency range are investigated using equation (15). In Figure 1 we have reported a comparison between the intensity noise spectra of the free-running laser and the injected laser for different values of the injected power. The spectra are calculated with the parameters corresponding to our experimental conditions listed in Table 1 and assuming a noiseless pump. Another significant effect of the injection is evident in Figure 1: the injection causes a very large reduction (depending on the injected power) of the excess noise in the frequency region around the relaxation oscillation peak. The strength of the relaxation oscillation peak is determined by the term $D(\tilde{\Omega})$ (Eq. (16)) which has the typical structure of a damped oscillator and appears in the denominator of equation (15). To understand the reason of the drastic reduction of the relaxation oscillation peak we have to compare $D(\tilde{\Omega})$ with the corresponding term for the free running laser, obtained by setting $x = 0$ in equation (16). Taking into account the relation verified between the different laser parameters, *i.e.* $a' \ll a \ll \tilde{\Omega}_{\mathrm{rel}} \ll x, b \ll 1$, where $\tilde{\Omega}_{\mathrm{rel}}$ is the dimensionless relaxation oscillation frequency, $D(\tilde{\Omega})$ can be written, for the injected laser, in a range of frequencies around $\tilde{\Omega}_{\mathrm{rel}}$, in the very simple following form:

$$D_{\mathrm{inj}}(\tilde{\Omega}) = b^2 \left| \tilde{\Omega}^2 - \mathrm{i}\frac{x}{2}\tilde{\Omega} - a(r-1) \right|^2. \qquad (21)$$

Starting from the same equation (16), setting $x = 0$ and making the same approximations, we can write for the free running laser:

$$D_{\mathrm{fr}}(\tilde{\Omega}) = b^2 \left| \tilde{\Omega}^2 + a\left[1 + (r-1)\frac{2}{b}\right] \mathrm{i}\tilde{\Omega} - a(r-1) \right|^2. \qquad (22)$$

The strong reduction of the relaxation oscillation peak in the injection locked laser is due to the very large damping term $\mathrm{i}(x/2)\tilde{\Omega}$ with respect to the free running laser, where the damping term is given by $a[1 + 2(r-1)/b]\mathrm{i}\tilde{\Omega}$. Assuming a very weak injected power, for example 10^{-4} times smaller than the free running emitted power, we have $x = 0.01$. A calculation with the parameters of our laser and with the normalised pump parameter $r = 4$ (a typical value used in the experiments) gives 2×10^{-4} for the damping term of the free running laser. The attenuation of the relaxation oscillation peak in the injected laser scales roughly as the square of the ratio between the corresponding damping terms. In this specific case the peak is decreased by about 30 dB. From the theoretical analysis it is clear that the combination of the principle of pump noise suppression with the injection locking is a very promising technique to obtain low intensity noise at the laser output. In fact we have shown that by injection locking it is possible to generate squeezed states for lower values of pump parameter r and to achieve better noise reduction in the low frequency region. The cancellation of the relaxation oscillation peak is also very important in order to improve the noise performances of these lasers in the low frequency region. In fact in a previous work [16] we have demonstrated the occurrence of non linear effects in the low frequency region of the noise spectra of these lasers in free running regime, due to the very large excess noise of the relaxation oscillation peak. The non linear effects result in an increase of the intensity noise at low frequency with respect to the theoretical predictions of the standard linear model based on quantum Langevin approach. The strong reduction of the relaxation oscillation peak should eliminate the extra noise in the low frequency region and allow to take advantage from the pump noise suppression. It is worth stressing that the investigation of these effects was not accessible in previous experiments which were dealing with Non Planar Ring Oscillator Nd:YAG lasers that are usually pumped by laser diode array, due to their relatively high oscillation threshold. The large intensity noise (typically more than 50 dB) exhibited by pump beam prevents to investigate these effects which result completely masked. In our case the choice of a microchip Nd:YVO_4 laser is determined by the necessity of having a low oscillation threshold which allows us to use a single element laser diode as a pump laser. The intensity noise of this kind of lasers can be reduced below the shot noise level applying well established techniques [1,3,19–23]. Our experimental set-up based on amplitude squeezed pump diode laser has been developed on the precise purpose of achieving operating regimes of the Nd:YVO_4 microchip laser suitable for the investigation of possible non-classical effects.

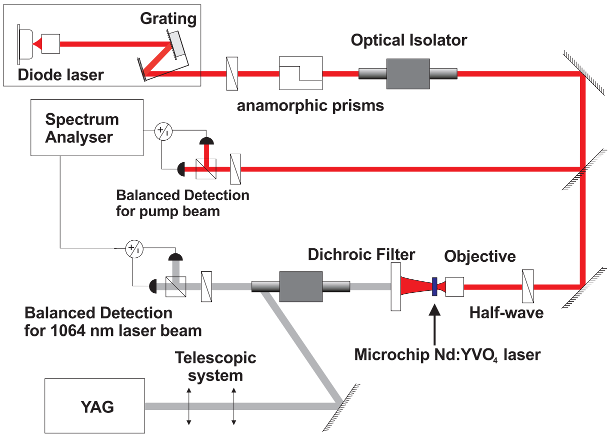

Fig. 3. Experimental set-up for noise measurements on the injected Nd:YVO$_4$ microchip laser.

3 Experimental set-up

The experimental set-up for the noise measurements on the injected Nd:YVO$_4$ microchip laser is shown in Figure 3. The amplitude squeezed diode laser used for optical pumping of solid state laser is an index guided quantum well GaAlAs laser diode (SDL 5422H1) operating at 810 nm. Noise reduction in the pump beam is achieved by driving the diode laser with a high impedance constant current source and suppressing the side modes using feedback from an external grating in an extended cavity laser [1,3,19–23]: by tilting the grating, the laser wavelength can be tuned to match the maximum of the Nd:YVO$_4$ line absorption at 808.5 nm. Astigmatism in the beam is corrected by means of anamorphic prisms. Two optical isolators (for a total isolation of 70 dB) are employed to prevent back reflection in the pump laser. The optical power available for pumping process is 45 mW (due to the losses of the grating): this allows us to operate the laser about 4 times above threshold. The intensity noise of the pump diode laser is measured by a standard balanced detection (two high efficiency EG&G FND100 PIN photodiodes), which allows to measure, under the same conditions, the shot noise and the intensity noise of the laser beam. We performed several tests in order to check the reliability of the shot noise measured in this way, as described in [23]. The common mode rejection of the balanced detection is better than 30 dB in the range of 0−30 MHz; electronic and dark noise are typically more than 10 dB below the shot noise level. The pump beam is sent to the microchip laser by mean of two mirrors and focused into the laser with a $f = 8$ mm objective. The polarisation of the pump beam is fixed by a half-wave plate in order to achieve the maximum absorption in the Nd:YVO$_4$ crystal. The microchip laser is mounted on a xyz-translation stage which allows an optimum alignment.

The Nd:YVO$_4$ microchip laser is 300 μm long, with a plane-plane monolithic cavity (the stability is ensured by thermal lens effects) in which the mirrors were deposited directly onto the crystal. The output mirror and back reflector have reflectivities of 97% and 99.5% respectively at 1.064 μm. The mirrors do not have special coatings for wavelength of pump radiation at 810 nm. Accurate measurements show a reflectivity of 24% and a transmissivity of 7% for pump radiation.

The injection locking was implemented by using a commercial Nd:YAG laser as the master laser. The frequency of the master laser is about 120 GHz below the Nd:YVO$_4$ laser frequency at room temperature. The frequency of the slave laser is tuned inside the injection locking bandwidth by heating the laser crystal. The temperature operation is around 100 °C; the temperature stabilisation by a PID control ensures variations less than 0.01 °C. The frequency shift *versus* the temperature for Nd:YVO$_4$ laser was found to be −1.6 GHz/°C (see also [24]): this implies that the jitter of the laser due to temperature variations is of the order of ten megahertz, and then negligible with respect to the observed injection bandwidth of about 200 MHz (the bandwidth calculated from the usual formula involving the cavity parameters, injected and emitted powers is expected to be 1 GHz). The master laser beam enters the output coupler of the slave laser through the escape port of an optical isolator which automatically match the polarisation of the master beam to the slave one; the Gaussian parameters of the master beam are reshaped with a telescopic lens system in order to have an efficient mode matching with the slave laser. The power effectively coupled into the slave laser is evaluated (from the observed injection bandwidth) to be 10% of the incident power, typically ranging between 100 to 500 μW. The emission wavelength of both the master and slave laser are measured by a high resolution monochromator. The injection locking is monitored with a Fabry-Perot analyser. With this experimental configuration we achieved a very stable injection locking operation over several hours.

For the intensity noise measurements on the emitted beam we used the following experimental set-up. For noise measurements up to 30 MHz, balanced detection is no longer reliable due to the very high excess noise of the relaxation peak (more than 80 dB) which exceeds the common mode rejection ratio (typically 30 dB). Therefore in this range of frequencies we choose to calibrate the shot noise level with an independent source. For the calibration we use the noise obtained by direct detection on one photodiode of attenuated radiation emitted by a shot noise limited diode laser. It is worth saying that no correction has to be calculated, due to the difference in the wavelength of the two beam. In fact we detect the noise of the photocurrent which is independent on the wavelength. We check carefully linear dependence of the calibrated shot noise signal with the optical power incident on the photodiode. The shot noise obtained in this way was in agreement within 0.1 dB with the noise obtained by a thermal light generating the same DC current on the photodiode.

4 Experimental results

In this section we present the experimental results obtained with the injected Nd:YVO$_4$ microchip laser previously described. In order to make a comparison between theory and experiment we have to determine all the parameters of the model. A set of values for the parameters describing the microchip laser (relaxations rates and cavity damping) has been determined in a previous work [11] in which an accurate investigation of the noise properties of the free-running laser is carried out. The experimental determination of the optical pump power threshold and the measurement of the optical pump power allows us to easily calculate the normalised pump parameter. With the laser operating at a temperature of 100 °C we have observed significant variations in the laser parameters with respect to the laser at room temperature. Assuming that the relaxation rates for the atomic populations and the atomic polarisation are virtually insensitive to temperature variations, the total cavity damping constant κ can be determined by the dependence of the relaxation oscillation frequency on the pump parameter r [11]. We have found for the total cavity damping $\kappa = 9 \times 10^9$ s^{-1}; the output coupling κ_{out}, calculated from the reflectivities of the cavity mirrors, is found to be 8.36×10^{-9}; the pump power threshold for oscillation is about 13 mW (4.2 mW at room temperature), the quantum efficiency of the pump mechanism 12.5% (40% at room temperature) and the maximum emitted power about 3.5 mW (10 mW at room temperature). We report in Table 1 the values of the parameters used in the numerical simulations. The sharp worsening of the performances of the Nd:YVO_4 microchip laser is strictly related to the heating of the crystal: in fact, as previously explained, this allows to tune the slave frequency at a rate of −1.6 GHz/°C; on the other hand the shift in the gain center frequency induced by heating is −0.53 GHz/°C [24]. The oscillating mode, at resonance with the center of the gain bandwidth at room temperature, is more and more detuned off resonance, as the temperature is increased. In our case, the total detuning from the gain center frequency (estimated to be 80 GHz) together with the FWHM gain bandwidth of the Nd:YVO_4 (257 GHz [24,25]) prevents us to obtain better performances from our laser.

We consider now the noise features of the master laser: our commercial laser is equipped with a standard feedback loop on the pump in order to eliminate the relaxation oscillation peak. Thus, the intensity noise spectrum at the output of the laser, for an emitted power of 700 mW, is rather flat over the whole range of observation (0−30 MHz) and exhibit an excess noise of 30 dB above the shot noise level (SNL). The theoretical model assumes that the injected field is in a coherent state *i.e.* with intensity noise limited to the SNL. However, in order to determine the intensity noise of the injected field, we have to take into account the linear optical losses that the beam emitted by the master laser undergoes before to be injected in the slave laser. Linear optical losses are usually modelled in quantum optics by a beam splitter with intensity transmission coefficient T. It can be shown that the effect of this attenuation on the intensity noise of the beam is expressed by the following equation (see for example [26]):

$$V_a(\widetilde{\Omega}) = 1 + T(V_b(\widetilde{\Omega}) - 1) \qquad (23)$$

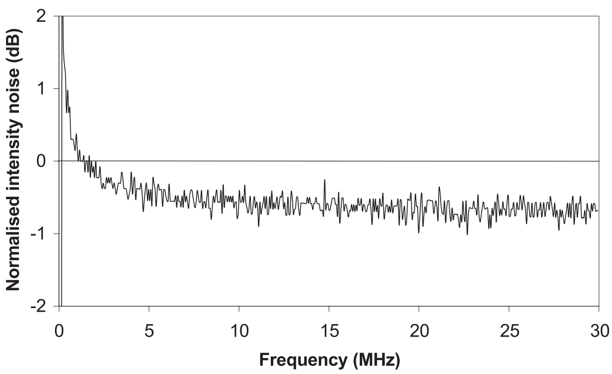

Fig. 4. Normalised intensity noise spectrum at the laser output (after correction for detection efficiency) for the grating extended cavity laser diode used as pump laser.

where V_a represents the normalised intensity noise of the beam after attenuation and V_b is the normalised intensity noise of the beam before attenuation; T is the optical attenuation. In our case the injected power is typically 0.1 mW, then $T = 0.1$ mW/700 mW $= 1.4 \times 10^{-4}$. It is evident from equation (23) that the intensity noise of the injected beam can be identified with the SNL with a very good approximation, according with the assumption of the model.

In the theoretical model the intensity noise of the Nd:YVO_4 microchip laser depends on the intensity noise of the pump beam. We use in the model the pump noise of the grating extended cavity diode laser, measured with high accuracy in [11] (see Fig. 4): after correction for detection efficiency the amount of amplitude squeezing at the laser output is 0.7 dB, flat over the whole frequency range between 1 to 20 MHz. For frequencies lower than 300 kHz the pump laser diode exhibits slight excess noise (<3 dB). For frequencies below 50 kHz technical $1/f$ noise increases the excess noise up to 10 dB.

The experimental results obtained with the injected Nd:YVO_4 microchip laser are shown in Figure 5. The graphic reports the normalised intensity noise spectra for different values of the injected master field amplitudes: good agreement is found between the predictions of the theoretical model (thick line) over a large range of frequencies. The parameters used in the calculations are reported in Table 1. As expected, the relaxation oscillation peak is completely damped (more than 60 dB of reduction with respect to the free-running laser) and the microchip laser exhibits a flat intensity noise spectrum with a noise level varying between 25 to 17 dB above the shot noise level, decreasing with the injected power.

The quite high excess noise is due to the poor laser features (namely high oscillation threshold and low quantum efficiency observed at high temperature); significant improvement is expected for injection locked laser operating at room temperature.

5 Conclusion

We have theoretically and experimentally investigated the noise properties of an injection locked diode pumped

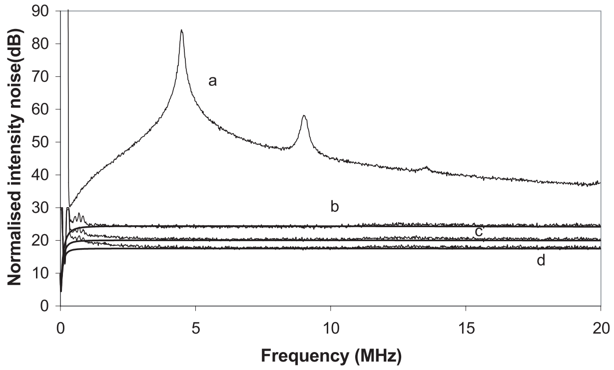

Fig. 5. Normalised experimental and theoretical (thick line) intensity noise spectra of the injected Nd:YVO$_4$ microchip laser for different injected powers (curve a: $x = 0$, curve b: $x = 0.16$, curve c: $x = 0.28$, curve d: $x = 0.36$). The parameters used in the calculations are given in the Table 1; normalised pump parameter is $r = 3.5$. The pump noise corresponds to the experimentally measured spectrum of the pump diode laser, shown in Figure 4.

Nd:YVO$_4$ microchip laser. The theoretical analysis clearly shows the effects of the injection: intensity squeezed light is achievable with lower pump parameters and the obtained noise reduction below the shot noise level are improved with respect to the free running regime. Moreover the relaxation oscillation peak is expected to be completely eliminated. The experimental intensity noise spectra confirm the theoretical predictions, showing that the injection technique allows to eliminate the relaxation oscillation peak, responsible for the huge excess noise that affect the spectrum of the free-running laser in the megahertz range. We found a good agreement between experimental results and theoretical calculations based on a fully quantum model describing the noise features of an injected laser. The minimum intensity noise obtained with this experimental configurations is 17 dB above the SNL. Further improvements could be achieved by implementing the injection locking at room temperature and increasing the pump rate in order to operate the microchip laser far above threshold.

Thanks are due to A.Z. Khoury, F. Marin and F. Prati for useful discussions and to Mr. Aubert, Molva and Fulbert from LETI/CEA for the loan of microlasers. This research was carried out in the framework of the EC ESPRIT Contract ACQUIRE no. 20029

Appendix

We report the non-vanishing diffusions coefficients for the c-number Langevin forces

$$2\mathcal{D}_{aa} = (\gamma_a + \gamma_a') \langle \mathcal{N}_a(t) \rangle + R(1-p) - g\left[\langle \mathcal{M}^*(t)\mathcal{A}(t) + \mathcal{A}^*(t)\mathcal{M}(t)\rangle\right] \quad (A.1)$$

$$2\mathcal{D}_{bb} = \gamma_b \langle \mathcal{N}_b(t) \rangle + \gamma_a' \langle \mathcal{N}_a(t) \rangle - g\left[\langle \mathcal{M}^*(t)\mathcal{A}(t) + \mathcal{A}^*(t)\mathcal{M}(t)\rangle\right] \quad (A.2)$$

$$2\mathcal{D}_{ab} = -\gamma_a' \langle \mathcal{N}_a(t) \rangle + g\left[\langle \mathcal{M}^*(t)\mathcal{A}(t) + \mathcal{A}^*(t)\mathcal{M}(t)\rangle\right] \quad (A.3)$$

$$2\mathcal{D}_{\mathcal{M}\mathcal{M}} = 2g \langle \mathcal{M}(t)\mathcal{A}(t) \rangle \quad (A.4)$$

$$2\mathcal{D}_{\mathcal{M}^*\mathcal{M}} = (2\gamma_{ab} - \gamma_a - \gamma_a') \langle \mathcal{N}_a(t) \rangle + R \quad (A.5)$$

$$2\mathcal{D}_{b\mathcal{M}} = \gamma_b \langle \mathcal{M}(t) \rangle \cdot \quad (A.6)$$

References

1. H. Wang, M.J. Freeman, D.G. Steel, Phys. Rev. Lett. **71**, 3951 (1993).
2. S. Inoue, S. Machida, Y. Yamamoto, H. Ozhu, Phys. Rev. A **48**, 2230 (1993).
3. F. Marin, A. Bramati, E. Giacobino, T.-C. Zhang, J.-Ph. Poizat, J.-F. Roch, P. Grangier, Phys. Rev. Lett. **75**, 4606 (1995).
4. A.C. Nilsson, IEEE J. Quant. Electron. **25**, 767 (1989).
5. A. Arie, S. Schiller, E.K. Gustafson, R.L. Byer, Opt. Lett. **17**, 1204 (1992).
6. I. Freitag, H. Welling, Appl. Phys. B **58**, 537 (1994).
7. T.C. Ralph, C.C. Harb, H.-A. Bachor, Phys. Rev. A **54**, 4359 (1996).
8. C.C. Harb, T.C. Ralph, E.H. Huntington, I. Freitag, D.E. McClelland, H.-A. Bachor, Phys. Rev. A **54**, 4370 (1996).
9. C. Becher, K.-J. Boller, Opt. Commun. **147**, 366 (1998).
10. C. Becher, K.-J. Boller, J. Opt. Soc. Am. B **16**, 286 (1999).
11. A. Bramati, J.P. Hermier, V. Jost, E. Giacobino, E. Molva, L. Fulbert, J.J. Aubert, Eur. Phys. J. D **6**, 513 (1999).
12. C.C. Harb, M.B. Gray, H.A. Bachor, R. Schilling, P. Rottengatter, I. Freitag, H. Welling, IEEE J. Quant. Electron. **30**, 2907 (1994).
13. M.S. Taubman, H. Wiseman, D.E. McClelland, H.A. Bachor, J. Opt. Soc. Am. B **12**, 1792 (1995).
14. E.H. Huntington, B.C. Buchler, C.C. Harb, T.C. Ralph, D.E. McClelland, H.-A. Bachor, Opt. Commun. **145**, 359 (1998).
15. B.C. Buchler, E.H. Huntington, C.C. Harb, T.C. Ralph, Phys. Rev. A **57**, 1286 (1998).
16. A. Bramati, J.P. Hermier, V. Jost, E. Giacobino, Phys. Rev. A **62**, 043806 (2001).
17. M. Fontenelle, L. Davidovich, Phys. Rev. A **51**, 2560 (1995).
18. C.C. Harb, T.C. Ralph, E.H. Huntington, D.E. McClelland, H.-A. Bachor, I. Freitag, J. Opt. Soc. Am. B **14**, 2936 (1997).
19. Yu.M. Golubev, I.V. Sokolov, Zh. Eksp. Teor. Phys. **87**, 804 (1984) [Sov. Phys. JETP **60**, 234 (1984)].
20. Y. Yamamoto, S. Machida, O. Nilsson, Phys. Rev. A **34**, 4025 (1986).
21. M.J. Freeman, H. Wang, D.G. Steel, R. Craig, D.R. Scifres, Opt. Lett. **18**, 2141 (1993).
22. M.J. Freeman, H. Wang, D.G. Steel, R. Craig, D.R. Scifres, Opt. Lett. **18**, 379 (1993).
23. T.-C. Zhang, J.-Ph. Poizat, P. Grelu, J.-F. Roch, P. Grangier, F. Marin, A. Bramati, V. Jost, M.D. Levenson, E. Giacobino, Quant. Semiclass. Opt. **7**, 601 (1995).
24. T. Taira, A. Mukai, Y. Nozawa, T. Kobayshi, Opt. Lett. **16**, 1955 (1991).
25. G.J. Kintz, T. Baer, IEEE J. Quant. Electron. **26**, 1457 (1990).
26. H.A. Bachor, *A Guide to experiments in Quantum Optics* (Wiley-VCH, 1998).